ACS APPLIED MATERIALS & INTERFACES

Research Article

www.acsami.org

Synthesis of Highly Efficient Flame Retardant High-Density Polyethylene Nanocomposites with Inorgano-Layered Double Hydroxides As Nanofiller Using Solvent Mixing Method

Yanshan Gao,[†] Qiang Wang,*[,†] Junya Wang,[†] Liang Huang,[†] Xingru Yan,[‡] Xi Zhang,[‡] Qingliang He,[‡] Zipeng Xing,[§] and Zhanhu Guo*[,‡]

[†]College of Environmental Science and Engineering, Beijing Forestry University, 35 Qinghua East Road, Haidian District, Beijing 100083, P. R. China

[‡]Integrated Composites Laboratory (ICL), Dan F. Smith Department of Chemical Engineering, Lamar University, Beaumont, Texas 77710, United States

[§]Key Laboratory of Functional Inorganic Material Chemistry, Ministry of Education of the People's Republic of China, Heilongjiang University, Harbin 150080, P. R. China

ABSTRACT: High-density polyethylene (HDPE) polymer nanocomposites containing $Zn_2Al–X$ (X= CO_3^{2-}, NO_3^-, Cl^-, SO_4^{2-}) layered double hydroxide (LDH) nanoparticles with different loadings from 10 to 40 wt % were synthesized using a modified solvent mixing method. Synthesized LDH nanofillers and the corresponding nanocomposites were carefully characterized using X-ray diffraction, scanning electron microscopy, and transmission electron microscopy, etc. The thermal stability and flame retardancy behavior were investigated using a thermo gravimetric analyzer and micro-scale combustion calorimeter. Comparing to neat HDPE, the thermal stability of nanocomposites was significantly enhanced. With the addition of 15 wt % $Zn_2Al–Cl$ LDH, the 50% weight loss temperature was increased by 67 °C. After adding LDHs, the flame retardant performance was significantly improved as well. With 40 wt % of LDH loading, the peak heat release rate was reduced by 24%, 41%, 48%, and 54% for HDPE/$Zn_2Al–Cl$, HDPE/$Zn_2Al–CO_3$, HDPE/$Zn_2Al–NO_3$, and HDPE/$Zn_2Al–SO_4$, respectively. We also noticed that different interlayer anions could result in different rheological properties and the influence on storage and loss moduli follows the order of SO_4^{2-} > NO_3^- > CO_3^{2-} > Cl^-. Another important finding of this work is that the influence of anions on flame retardancy follows the exact same order on rheological properties.

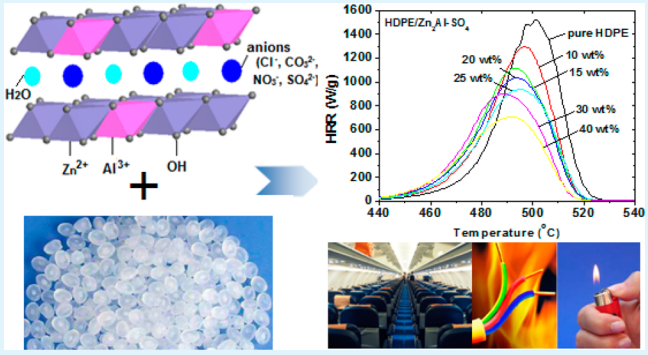

KEYWORDS: *inorganic anions, nanocomposites, solvent mixing, thermal stability, flame retardancy, rheology*

1. INTRODUCTION

High density polyethylene (HDPE) has good electrical properties, high stiffness, and tensile strength, especially high dielectric strength of the insulation, making it very suitable for wires and cables. However, one problem for HDPE is that it is combustible and flame retardation is needed in many applications.[1−5] For instance, when HDPE was used as insulating materials for wires and cables, both the superior high-heat resistance and the flame-retardant properties are required for some special applications. Another large market for flame retardant HDPE is for the replacement of wooden pallets and crates.[6] In order to improve the flame-retardant properties of polymers, many organic and inorganic flame retardants have been developed, for instance, halogenated organic compounds, magnesium hydroxide, aluminum hydroxide, and metal borates, etc.[7−9] However, new environmental regulations have restricted the use of some halogenated flame-retardant additives, which could produce a large amount of smoke and toxic gases during burning.[10] One of the fast growing classes of halogen-free flame retardants is aluminum hydroxide ($Al(OH)_3$, ATH) and magnesium hydroxide ($Mg(OH)_2$, MDH). These two metal hydroxides are now widely used as flame retardants in wire coatings on cables and in building and construction applications. Although, these materials offer a cost-effective solution for flame retardancy, they have some drawbacks. The most important one is that a very high loading is needed to achieve the flame-retardant rating of the products. Alumina trihydrate (ATH) and magnesium hydroxide (MDH) are typically added in the amount of 50−70 wt % to the polymer. As a consequence, the mechanical properties of the polymer compound are deteriorated and the processing becomes difficult.[11] Thus, some alternative flame retardant materials

Received: January 14, 2014
Accepted: March 5, 2014
Published: March 5, 2014

   dx.doi.org/10.1021/am500265a | *ACS Appl. Mater. Interfaces* 2014, 6, 5094−5104

which are environmentally friendly and more efficient are highly desired.

Layered double hydroxides (LDHs), also commonly called anionic clays, are a class of anionic lamellar compounds made up of positively charged brucite-like layers with an interlayer region containing charge compensating anions and solvation molecules. LDHs have a general molecular formula of $[M_{1-X}^{2+}M_X^{3+}(OH)_2]^{X+}A_{x/m}^{n-}\cdot nH_2O$, where M^{2+} is divalent metal cations such as Mg^{2+}, Zn^{2+}, Cu^{2+}, and Ca^{2+}, and M^{3+} is trivalent metal cations such as Al^{3+}, Fe^{3+}, and Mn^{3+}; A^{n-} is an intercalated inorganic or organic anions such as CO_3^{2-}, NO_3^-, SO_4^{2-}, borate, and stearate, etc; and x is normally between 0.2 and 0.4.[12−14] Because of their layered structure and high anion exchange capacity, LDHs are now used in various applications, such as precursors for preparing CO_2 adsorbents,[15−21] catalysts,[22,23] fire retardant additives,[24,25] UV absorbents,[26,27] drug delivery hosts,[28] as cement additives,[29] and so on. Recently, LDHs have attracted increasing attention as a new generation of flame-retardant material. LDHs have been shown to offer good flame retardancy and smoke suppression properties due to their unique chemical composition and layered structure.[30,31] During combustion, LDHs lose the interlayer water, intercalated anions, and dehydroxylate to mixed metal oxides. These processes absorb huge amounts of heat, dilute the concentration of O_2, promote the formation of an expanded carbonaceous coating or char on the polymer, protecting the bulk polymer from being exposed to air, and suppress smoke production due to suffocation.[11,32−35] Therefore, LDHs have been regarded as a promising new type of environmental friendly and highly efficient flame retardant for polymer applications.

Because of the fact that LDHs have strong interlayer electrostatic interactions, small gallery spaces, and hydrophilic properties, it is generally believed that pristine LDHs should be modified with different organic modifiers to alter their surface properties, expand their basal spacing, and facilitate their interactions with polymers.[36] For this reason, until now most of the LDHs used as flame retardant additives for polymers are organic anions intercalated LDHs, such as LDH-alkyl carboxylates,[24] LDH-dodecylbenzenesulfonate,[34] LDH-dodecyl sulfate,[37] LDH-oleate,[38,39] LDH-undecenoate,[13,40] etc. Although there are a few papers using inorganic anions intercalated LDHs as flame retardant additives, all of them were prepared using the melt mixing method.[41−43] One drawback of melt mixing is the drying of LDHs dispersion before melt mixing inevitably results in LDHs particle aggregation, resulting in inferior LDHs dispersion compared to the solvent-based synthesis. Until recently, it was widely believed that the inorganic-LDHs containing inorganic anions such as CO_3^{2-}, NO_3^-, SO_4^{2-}, and Cl^- cannot be dispersed in nonpolar solvents due to their high hydrophilicity.[44] For this reason, there is still no report on the comparison of the influence of inorganic anions on the flame retardancy of polymer nanocomposites, particularly for those synthesized using the solvent mixing method.

Recently, we have developed an aqueous miscible organic solvent treatment (AMOST) method for the synthesis of stable, transparent dispersions of the hydrophilic LDHs in nonpolar solvents.[44,45] This technique can tune the surface of LDHs to be hydrophobic, enable them to be highly dispersible in nonpolar solvents such as xylene, and make it possible to prepare polyolefin/inorgano-LDHs nanocomposites using solvent mixing method for the first time ever. By taking the advantages of this great breakthrough, we are now able to introduce highly dispersed inorganic anions intercalated LDHs into HDPE and compare their influence on the flame retardant performance of HDPE nanocomposites.

In this paper, the HDPE nanocomposites filled with different inorganic anions (CO_3^{2-}, SO_4^{2-}, NO_3^-, and Cl^-) intercalated LDHs were prepared using the solvent mixing method for the first time. The loadings of LDHs were controlled within 10−40 wt %, and both LDHs and HDPE nanocomposites were carefully characterized. Then the influence of interlayer anions on the thermal stability, flame retardancy, and rheological properties of HDPE nanocomposites were evaluated in detail.

2. EXPERIMENTAL SECTION

2.1. Synthesis of LDHs and HDPE/LDH Nanocomposites. Zn_2Al−X LDH was synthesized by a traditional coprecipitation method.

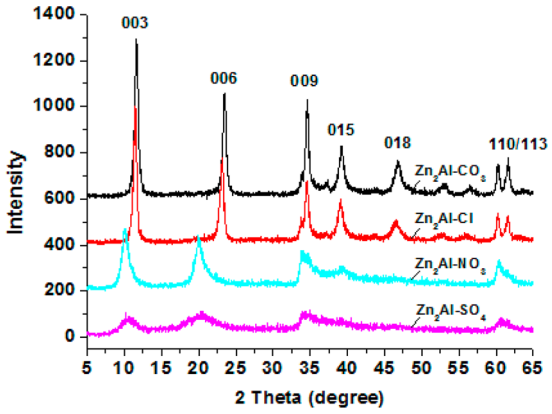

Figure 1. XRD patterns of Zn_2Al−X (X = CO_3^{2-}, Cl^-, NO_3^-, and SO_4^{2-}) LDHs washed with acetone.

In brief, Zn_2Al−CO_3 LDH was prepared by adding 50 mL of solution containing 7.44 g of $Zn(NO_3)_2\cdot 6H_2O$ (0.025 mol) and 4.7 g of $Al(NO_3)_3\cdot 9H_2O$ (0.0125 mol) solution dropwise into a 50 mL solution containing 2.65 g of Na_2CO_3 (0.025 mol) solution. The pH of the precipitation solution was controlled at ∼10 using a NaOH (4 M) solution. Zn_2Al−NO_3 LDH was synthesized in the same way, with an only exception that the Zn_2Al solution was added dropwise into a 50 mL solution containing 2.125 g of $NaNO_3$ (0.025 mol). Similarly, Zn_2Al−Cl and Zn_2Al−SO_4 were prepared by adding a $ZnCl_2$ and $AlCl_3\cdot 6H_2O$ (or $ZnSO_4\cdot 7H_2O$ and $Al_2(SO_4)_3\cdot 18H_2O$) solution into a NaCl (or Na_2SO_4) solution, with the pH controlled at 10 using a 4 M NaOH solution. The obtained LDHs were washed with H_2O until pH = 7. The sample was further washed with acetone intensively. Finally all the samples were dried in an oven at 65 °C for overnight to obtain the LDH powders. For the preparation of HDPE/LDH nanocomposites, the acetone washed slurries were directly used without drying.

HDPE was purchased from Dow Chemical Company (density, 0.942 g cm^{-1}; melt index, 2; and melting temperature, 127 °C). The HDPE/Zn_2Al−X LDH nanocomposites were prepared using a solvent mixing method. In brief, 5 g of HDPE, the acetone washed LDH slurry prepared above, and 100 mL of xylene were charged into a 250-mL round-bottom flask. The amount of LDH added (corresponding to pure HDPE) is 10, 15, 20, 25, 30, and 40 wt %, respectively. The mixture was refluxed at approximately 140 °C for 2 h. After the reflux process was complete, the hot xylene solution containing dissolved HDPE and highly dispersed LDH nanoparticles was poured into a crystallizing dish. The obtained HDPE/LDH nanocomposites were then dried in vacuum.

2.2. Characterization of LDHs. *X-ray Diffraction (XRD).* XRD patterns were recorded on a Shimadzu XRD-6000 instrument in reflection mode with Cu Kα radiation. The accelerating voltage was set at 40 kV with 30 mA current (λ = 1.542 Å) at 0.1° s^{-1} from 5 to 65°.

Scanning Electron Microscope (FE-SEM). Field emission (FE)-SEM analyses were performed on a SU-8020 scanning microscope with an accelerating voltage of 5.0 kV. Powder samples were spread on carbon

dx.doi.org/10.1021/am500265a | ACS Appl. Mater. Interfaces 2014, 6, 5094−5104

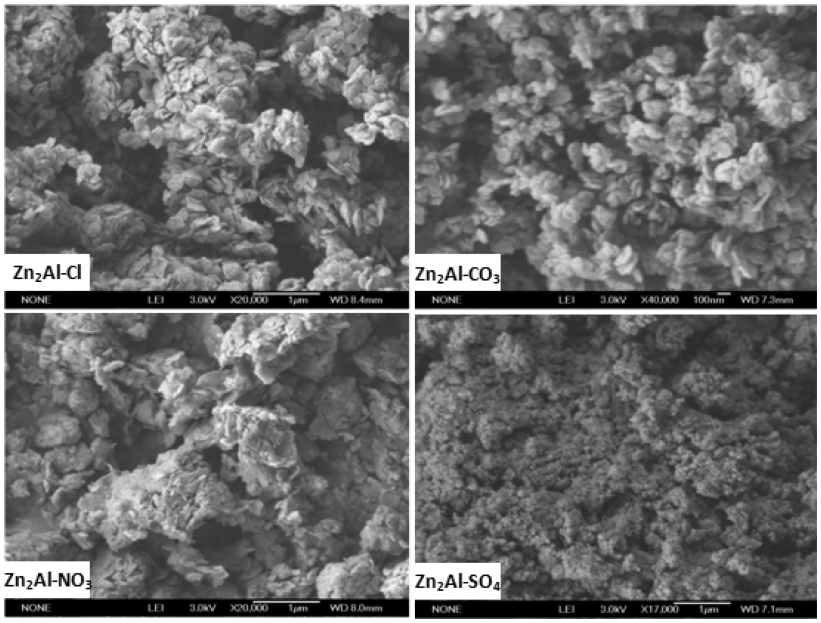

Figure 2. FE-SEM images of Zn_2Al-Cl, Zn_2Al-CO_3, Zn_2Al-NO_3, and Zn_2Al-SO_4 LDHs.

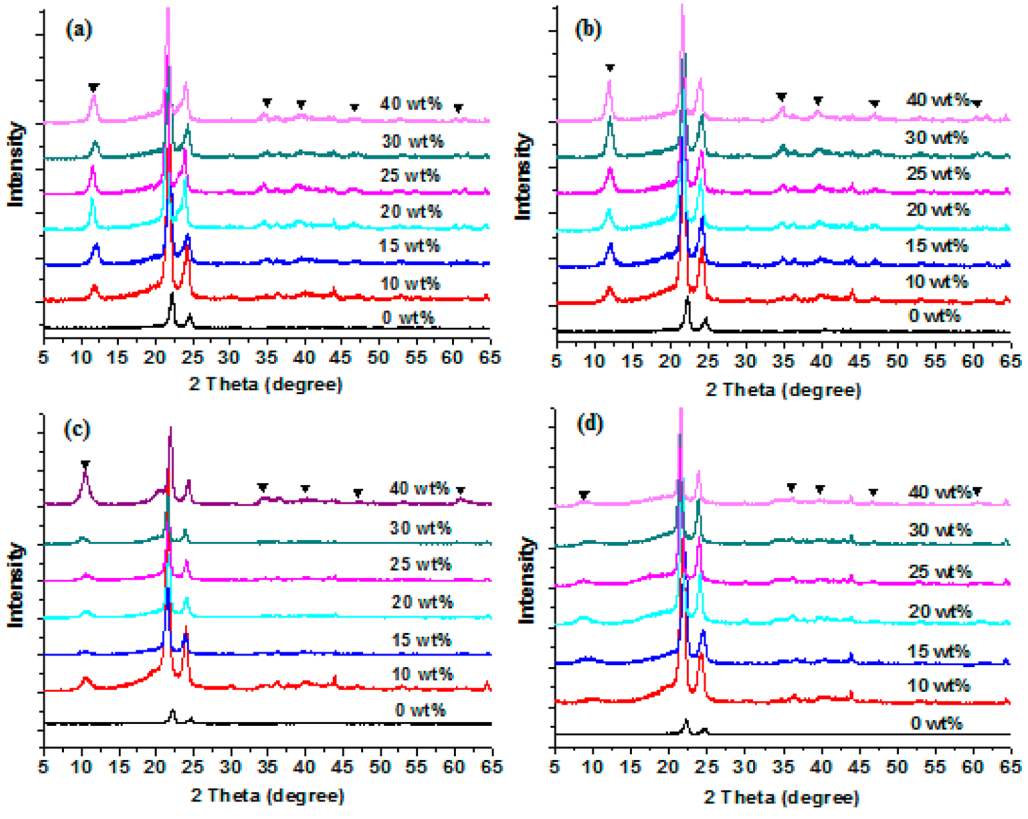

Figure 3. XRD patterns of (a) HDPE/Zn_2Al-Cl LDH nanocomposites (b) HDPE/Zn_2Al-CO_3 LDH nanocomposites (c) HDPE/Zn_2Al-NO_3 LDH nanocomposites (d) HDPE/Zn_2Al-SO_4 LDH nanocomposites.

tape adhered to the SEM stage. Before observation, the samples were sputter coated with a thin platinum layer to prevent charging and to improve the image quality.

2.3. Thermal Stability and Rheological Property of HDPE/LDHs. *Thermal Gravimetric Analysis (TGA).* The thermal stability of all the samples was evaluated using TGA (TGA 50, TA Instrument), which was carried out with a heating rate of 10 °C min^{-1} and an air flow rate of 50 mL min^{-1} from 25 to 600 °C.

Microscale Combustion Calorimeter (MCC-2). MCC-2 was used to investigate the combustion behavior of the synthesized HDPE nanocomposites. In this system, about 5 mg samples were heated to 700 °C at a heating rate of 1 °C s^{-1} in a stream of nitrogen flowing at 80 cm^3 min^{-1}. The volatile, anaerobic thermal degradation products in the nitrogen gas stream were mixed with a 20 cm^3 min^{-1} stream of 20% oxygen and 80% nitrogen prior to entering a 900 °C combustion furnace. The parameters measured from this test are heat release rate (HRR) in W g^{-1} (calculated from the oxygen depletion measurements),

dx.doi.org/10.1021/am500265a | ACS Appl. Mater. Interfaces 2014, 6, 5094−5104

heat release capacity (HRC) in J g^{-1} K^{-1} (obtained by dividing the sum of the peak HRR by the heating rate in K s^{-1}), the total heat release (THR) in kJ g^{-1} (given by integrating the HRR curve).

Rheological Behavior. The melt rheological behavior of neat HDPE and its nanocomposites were studied using a TA Instruments AR 2000ex Rheometer. An environmental test chamber (ETC) steel parallel-plate geometry (25 mm in diameter) was used to perform the measurement at 200 °C when HDPE was in the melt state. The frequency sweep was from 100 to 0.1 Hz in the linear viscoelastic (LVE) range (strain 1%) under a nitrogen atmosphere to prevent the oxidation of HDPE.

3. RESULTS AND DISCUSSION

3.1. Characterization of LDHs. The synthesized Zn_2Al-X LDHs were first characterized using XRD analysis, Figure 1. The

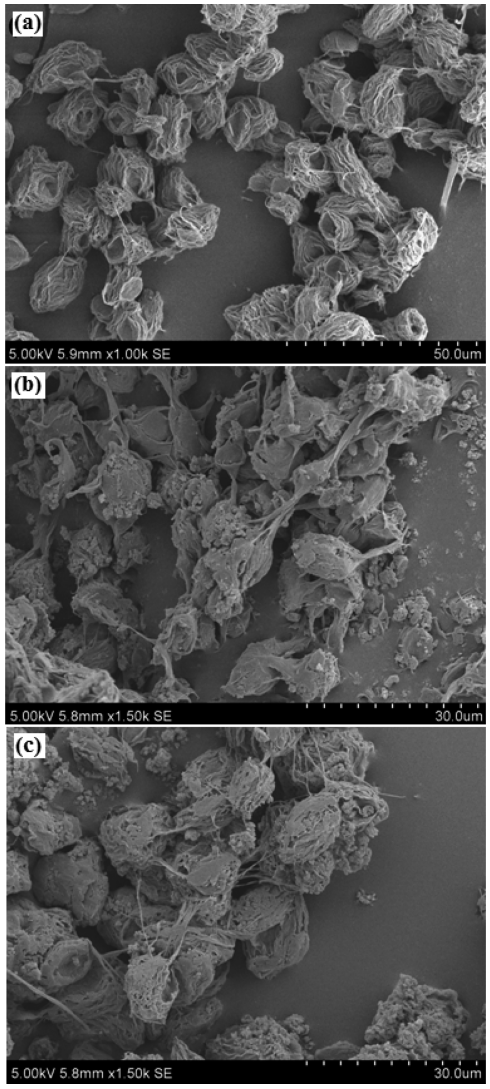

Figure 4. SEM images of (a) neat HDPE and HDPE/Zn_2Al-SO_4 nanocomposites with a LDH loading of (b) 15 and (c) 30 wt %.

XRD patterns for all LDH samples exhibit the typical patterns of hydrotalcite-like materials. The characteristic reflections of (003), (006), (009), (015), (018), and (110/113) planes are observed for all Zn_2Al-X LDHs, suggesting that all of the LDHs had a well-developed layer structure. A slight difference in the interlayer distance is observed when various anions were used, probably due to the difference in their dimension and carried charges.[19] For Zn_2Al-CO_3, the characteristic reflections of (003) is observed at 11.68°, corresponding to an interlayer distance of 0.76 nm. Zn_2Al-Cl has a similar interlayer distance with a calculated value of 0.77 nm. However, when the interlayer anions are NO_3^- and SO_4^{2-}, the interlayer distances are enlarged to be 0.85 and 0.87 nm, respectively. The XRD patterns also indicate that Zn_2Al-CO_3 and Zn_2Al-Cl LDHs have sharper basal reflections, suggesting a higher crystalline degree for those two nanoparticles. The basal reflections of Zn_2Al-SO_4 and Zn_2Al-NO_3 LDHs are much weaker, suggesting the formation of less crystallized nanoparticles.

The morphologies of Zn_2Al-X LDHs were then characterized using FE-SEM analysis, Figure 2. The images of Zn_2Al-Cl and Zn_2Al-CO_3 show that both of them have formed platelike nanoparticles with regular shape, as commonly observed for the typical inorganic anionic intercalated LDH compounds.[46] The layer nanoparticles have a diameter over a few hundred nanometers and a thickness over several tens of nanometers. However, no regular nanoplates are observed for Zn_2Al-NO_3 and Zn_2Al-SO_4, suggesting that the crystalline degree of these two LDHs is lower than that of Zn_2Al-Cl and Zn_2Al-CO_3. This result is consistent with the XRD analysis.

3.2. Characterization of HDPE/LDH Nanocomposites. After introducing LDHs into HDPE, the obtained HDPE/Zn_2Al-X LDH nanocomposites with various loadings of 0−40 wt % were first characterized using XRD analysis, Figure 3. For pure HDPE, two characteristic reflections at 22.26 and 24.66° corresponding to the (110) and (200) planes are observed, which is consistent with the reports from the literature.[47,48] After adding LDHs, several new XRD peaks which can be attributed to the characteristic reflections of (003), (009), (015), (018), and (110/113) planes of LDHs are clearly observed for all the HDPE/Zn_2Al-X LDH nanocomposites. With increasing the LDH loading, the intensity of the (00l) reflection is gradually increased. These results clearly indicate that the LDHs nanoparticles have been successfully introduced into the HDPE matrix using the solvent method.

The morphology of the synthesized nanocomposites was further examined by SEM analysis. Figure 4 shows the SEM images of pure HDPE and its Zn_2Al-SO_4 nanocomposites with a LDH loading of 15 and 30 wt %. Spherical particles with an average size of about ∼10 μm were formed for pure HDPE and all the HDPE/Zn_2Al-SO_4 LDH nanocomposites. Pure HDPE shows a smooth surface while a few LDH nanoparticles can be observed on the surface of HDPE/LDH nanocomposites. And the number of surface LDHs nanoparticles increases with increasing the LDH loading from 15 to 30 wt %. This is reasonable since the LDH loading is relatively high in these HDPE nanocomposites.

3.3. Performance Test of HDPE/LDH Nanocomposites. Since LDH nanofillers may affect the thermal stability of HDPE, the influence of different anions intercalated LDHs on the thermal stability of HDPE was further investigated using TGA, Figure 5. The corresponding detailed data are also summarized in Table 1. The pristine HDPE is observed to begin to decompose at around 330−340 °C under air atmosphere, which can be apparently referred to the chemical composition of its main chains. HDPE chain can easily undertake oxygen insertion reaction when it is exposed to air at elevated temperatures. Then it could form peroxy radical species and other oxidized species at elevated temperatures. All these reactions have weakened the thermal stability of the main chains of HDPE, which starts to generate gaseous products under the air atmosphere at approximately 330−340 °C, thus leading to the weight loss.[49]

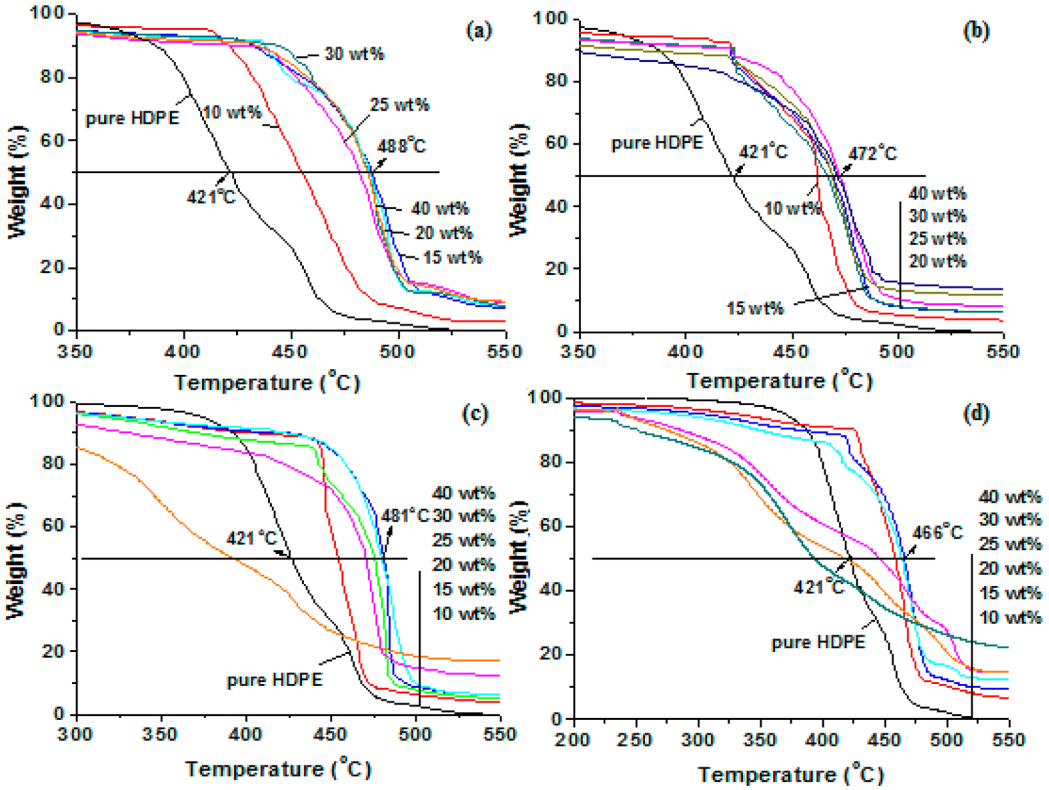

Figure 5. TGA curves of (a) HDPE/Zn_2Al−Cl LDH nanocomposites, (b) HDPE/Zn_2Al−CO_3 LDH nanocomposites, (c) HDPE/Zn_2Al−NO_3 LDH nanocomposites, and (d) HDPE/Zn_2Al−SO_4 LDH nanocomposites.

Table 1. TGA Summary Results of Pure HDPE and Its Nanocomposites[a]

sample	$T_{0.1}$	$\Delta T_{0.1}$	$T_{0.5}$	$\Delta T_{0.5}$
HDPE	387	NA	421	NA
HDPE-10 wt % Zn_2Al−Cl	421	34	455	34
HDPE-15 wt % Zn_2Al−Cl	432	45	488	67
HDPE-20 wt % Zn_2Al−Cl	438	51	487	66
HDPE-25 wt % Zn_2Al−Cl	428	41	482	61
HDPE-30 wt % Zn_2Al−Cl	444	57	486	65
HDPE-40 wt % Zn_2Al−Cl	435	48	486	65
HDPE-10 wt % Zn_2Al−CO_3	422	35	462	41
HDPE-15 wt % Zn_2Al−CO_3	421	34	469	48
HDPE-20 wt % Zn_2Al−CO_3	423	36	466	45
HDPE-25 wt % Zn_2Al−CO_3	421	34	472	51
HDPE-30 wt % Zn_2Al−CO_3	377	−10	468	47
HDPE-40 wt % Zn_2Al−CO_3	344	−43	471	50
HDPE-10 wt % Zn_2Al−NO_3	403	16	454	33
HDPE-15 wt % Zn_2Al−NO_3	409	22	475	54
HDPE-20 wt % Zn_2Al−NO_3	421	34	481	60
HDPE-25 wt % Zn_2Al−NO_3	421	34	480	59
HDPE-30 wt % Zn_2Al−NO_3	329	−58	470	49
HDPE-40 wt % Zn_2Al−NO_3	258	−129	392	−29
HDPE-10 wt % Zn_2Al−SO_4	419	32	458	37
HDPE-15 wt % Zn_2Al−SO_4	375	−12	466	45
HDPE-20 wt % Zn_2Al−SO_4	348	−39	464	43
HDPE-25 wt % Zn_2Al−SO_4	286	−101	446	25
HDPE-30 wt % Zn_2Al−SO_4	273	−114	421	0
HDPE-40 wt % Zn_2Al−SO_4	250	−137	393	−28

[a] $T_{0.1}$ = temperature of 10% mass loss; $T_{0.5}$ = temperature of 50% mass loss; and ΔT = difference between virgin polymer and its nanocomposite.

From 330 to 340 °C to around 550 °C, HDPE experiences a fast oxidative degradation till only very little residue is left.[34,50,51]

However, the thermal oxidative degradation of the HDPE/Zn_2Al−X LDH nanocomposites experienced differently compared with that of neat HDPE. The 10% weight loss temperatures ($T_{0.1}$), the 50% weight loss temperature, and the corresponding temperature increase (or decrease) in $T_{0.1}$ and $T_{0.5}$ of the HDPE/Zn_2Al−X LDH nanocomposites are summarized in Table 1. It is obvious that the addition of the Zn_2Al−X LDHs to HDPE significantly improves the thermal stability of HDPE, particularly when the LDH loading is low. In general, both $T_{0.1}$ and $T_{0.5}$ are first increased with increasing the LDH loading and then slightly decreased with a further increase in the LDH loading. For instance, the maximum temperature increase (67 °C) in $T_{0.5}$ for the HDPE/Zn_2Al−Cl LDH nanocomposites is observed with 15 wt % loading, with $T_{0.5}$ increased from 421 °C for neat HDPE to 488 °C for nanocomposites. With a further increase in LDH loading up to 40 wt %, the temperature increase in $T_{0.5}$ is still very high, ~65 °C. For the other three nanocomposites of HDPE/Zn_2Al−CO_3, HDPE/Zn_2Al−NO_3, and HDPE/Zn_2Al−SO_4, the maximum temperature increase in $T_{0.5}$ is observed with 20−25 wt % LDH loading, which is ~51, 60, and 45 °C, respectively. For HDPE/Zn_2Al−Cl and HDPE/Zn_2Al−CO_3 LDH nanocomposite, even the LDH loading is as high as 40 wt %, the $T_{0.5}$ increase is still very high (~65 and 50 °C). On the contrary, for HDPE/Zn_2Al−NO_3 and HDPE/Zn_2Al−SO_4 LDH nanocomposites, when the LDH loading is increased up to 40 wt %, the $T_{0.5}$ is decreased by 29 and 28 °C, respectively. These results obviously suggest that the LDH nanofillers can significantly increase the thermal stability of HDPE but different LDHs would lead to different performance, which should be considered for practical applications. Regarding

dx.doi.org/10.1021/am500265a | ACS Appl. Mater. Interfaces 2014, 6, 5094−5104

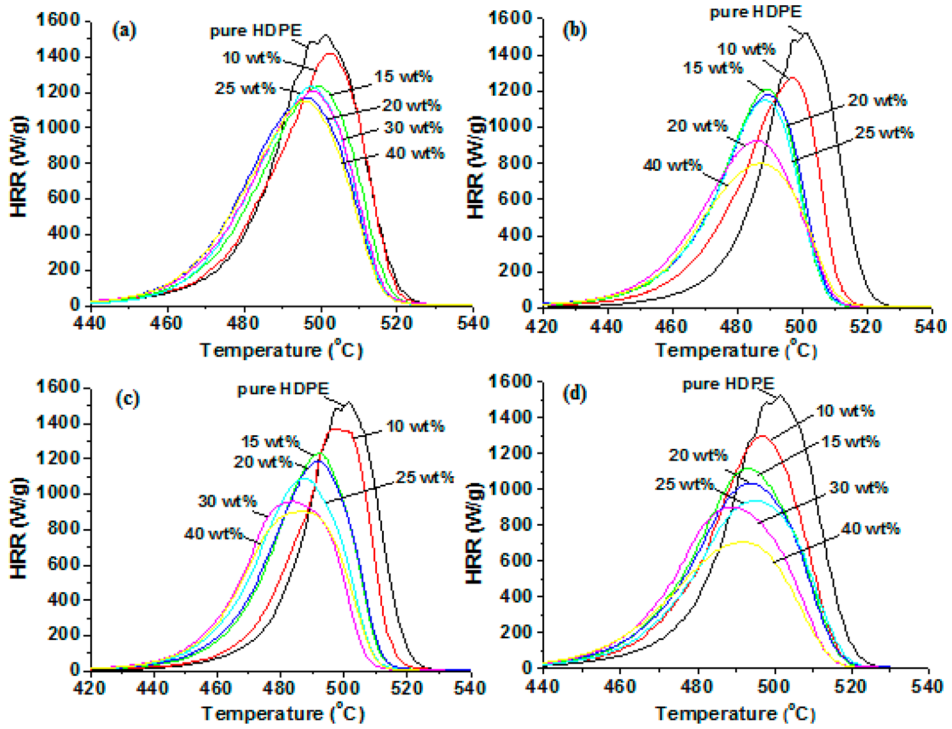

Figure 6. MCC analysis of (a) HDPE/Zn_2Al−Cl LDH nanocomposites, (b) HDPE/Zn_2Al−NO_3 LDH nanocomposites, (c) HDPE/Zn_2Al−CO_3 LDH nanocomposites, and (d) HDPE/Zn_2Al−SO_4 LDH nanocomposites.

Table 2. Data Recorded in MCC-2 Measurement for HDPE and Its Nanocomposites[a]

sample	PHRR/W g^{-1}	reduction/%	THR/K J g^{-1}	T_{max}/°C	HRC/J g^{-1} K^{-1}
HDPE	1521	NA	41.5	416	1540
HDPE-10 wt % Zn_2Al−Cl	1418	7	39.0	420	1330
HDPE-15 wt % Zn_2Al−Cl	1230	19	36.8	418	1164
HDPE-20 wt % Zn_2Al−Cl	1170	23	35.7	412	1186
HDPE-25 wt % Zn_2Al−Cl	1230	19	35.5	414	1162
HDPE-30 wt % Zn_2Al−Cl	1207	21	37.7	416	1132
HDPE-40 wt % Zn_2Al−Cl	1150	24	35.4	413	1079
HDPE-10 wt % Zn_2Al−CO_3	1371	10	37.7	415	1290
HDPE-15 wt % Zn_2Al−CO_3	1226	19	36.3	410	1130
HDPE-20 wt % Zn_2Al−CO_3	1184	22	36.2	408	1122
HDPE-25 wt % Zn_2Al−CO_3	1085	29	35.6	404	1045
HDPE-30 wt % Zn_2Al−CO_3	959	37	33.3	402	903
HDPE-40 wt % Zn_2Al−CO_3	898	41	32.9	403	850
HDPE-10 wt %Zn_2Al−NO_3	1348	11	36.7	414	1280
HDPE-15 wt % Zn_2Al−NO_3	1226	19	34.7	412	1157
HDPE-20 wt % Zn_2Al−NO_3	1179	23	35.3	407	1110
HDPE-25 wt % Zn_2Al−NO_3	1150	24	34.0	405	1090
HDPE-30 wt % Zn_2Al−NO_3	922	39	32.8	404	875
HDPE-40 wt % Zn_2Al−NO_3	791	48	29.3	406	749
HDPE-10 wt % Zn_2Al−SO_4	1296	15	37.1	415	1224
HDPE-15 wt % Zn_2Al−SO_4	1137	25	35.7	414	1070
HDPE-20 wt % Zn_2Al−SO_4	1034	32	33.8	410	975
HDPE-25 wt % Zn_2Al−SO_4	936	39	31.7	412	886
HDPE-30 wt % Zn_2Al−SO_4	894	41	30.6	405	847
HDPE-40 wt % Zn_2Al−SO_4	706	54	25.8	407	669

[a]HRC = heat release rate; THR = total heat release; PHRR = peak heat release rate; T_{max} = temperature at maximum pyrolysis rate.

the thermal stability enhancement, the efficiency of LDHs follows the order of Zn_2Al−Cl > Zn_2Al−CO_3 > Zn_2Al−NO_3 > Zn_2Al−SO_4.

MCC measures the flammability of materials on milligram quantities and is based on the principle of oxygen consumption. It is a small-scale flammability testing technique to screen polymer flammability prior to scale-up and is a convenient, fast, and relatively new technique for laboratory evaluation of the flame properties. It was regarded as one of the most effective methods for investigating the combustion properties of polymer

dx.doi.org/10.1021/am500265a | ACS Appl. Mater. Interfaces 2014, 6, 5094−5104

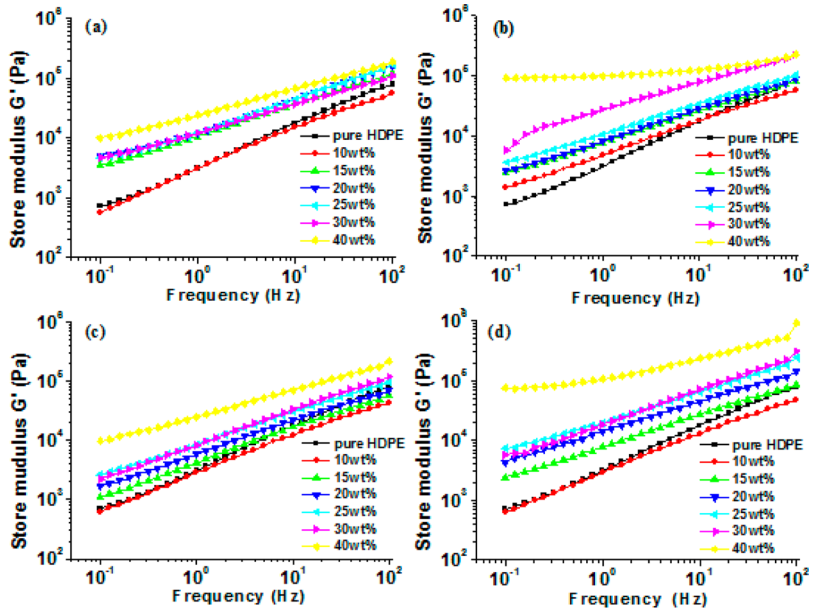

Figure 7. Graphs of G′ (storage modulus) vs frequency for neat HDPE and (a) HDPE/Zn_2Al−Cl LDH nanocomposites, (b) HDPE/Zn_2Al−NO_3 LDH nanocomposites, (c) HDPE/Zn_2Al−CO_3 LDH nanocomposites, and (d) HDPE/Zn_2Al−SO_4 LDH nanocomposites.

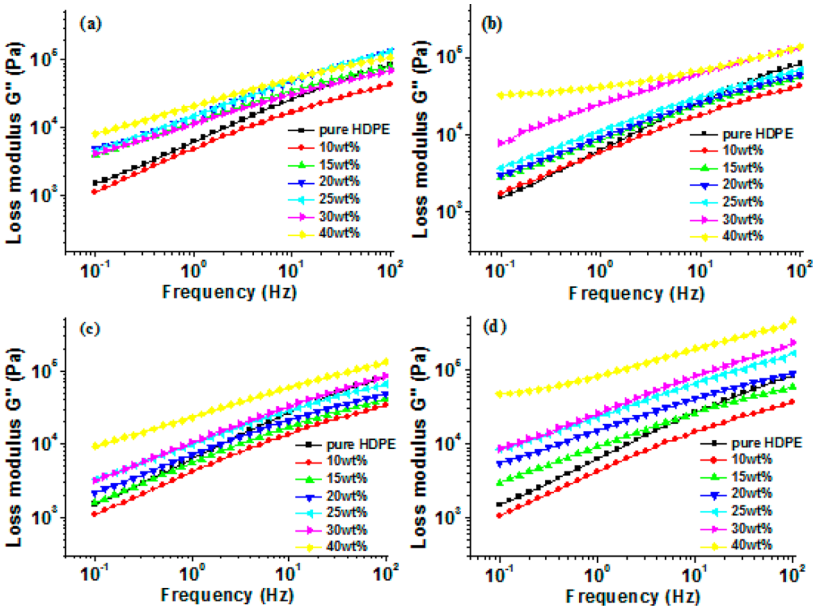

Figure 8. Graphs of G″ (loss modulus) vs frequency for neat HDPE and (a) HDPE/Zn_2Al−Cl LDH nanocomposites, (b) HDPE/Zn_2Al−NO_3 LDH nanocomposites, (c) HDPE/Zn_2Al−CO_3 LDH nanocomposites, and (d) HDPE/Zn_2Al−SO_4 LDH nanocomposites.

materials.[52−54] In the case of MCC measurement, the heat is produced via full combustion of the fuel gases generated during the pyrolysis of samples, showing several parameters, such as specific heat release rate (HRR), heat release capacity (HRC), total heat release (THR), etc. These parameters are very important to reflect the combustion properties of materials and allow a reasonable estimation of the fire hazard using small quantities of samples.[55]

Figure 6 presents the HRR curves of pure HDPE and HDPE/Zn_2Al−X LDH nanocomposite, and the related combustion parameters are summarized in Table 2. It is obvious that the peak heat release rate (PHRR) values of all the HDPE/Zn_2Al−X LDH nanocomposites are much lower than that of neat HDPE. For all the HDPE/Zn_2Al−X LDH nanocomposites, the reduction in PHRR increases with increasing the LDH loading. For neat HDPE, the PHRR value is ∼1521 W g^{-1}. After adding 40 wt % LDHs, the PHRR value is reduced by 24%, 41%, 48%, and 54% for Zn_2Al−Cl, Zn_2Al−CO_3, Zn_2Al−NO_3, and Zn_2Al−SO_4, respectively. Compared to Zn_2Al−Cl, the other three LDHs Zn_2Al−CO_3, Zn_2Al−NO_3, and Zn_2Al−SO_4 have a much higher efficiency on improving the flame retardancy of HDPE. These results clearly indicate that the Zn_2Al−X LDHs can significantly improve the flame retardant performance of HDPE. Also, different interlayered anions in LDHs have different flame retardant efficiency, which follows the order of SO_4^{2-} > NO_3^- > CO_3^{2-} > Cl^-. The mechanism of Zn_2Al−X LDH in reducing the flammability of HDPE can probably be attributed to the creation of a barrier effect on the surface of polymers, which slows down

dx.doi.org/10.1021/am500265a | ACS Appl. Mater. Interfaces 2014, 6, 5094−5104

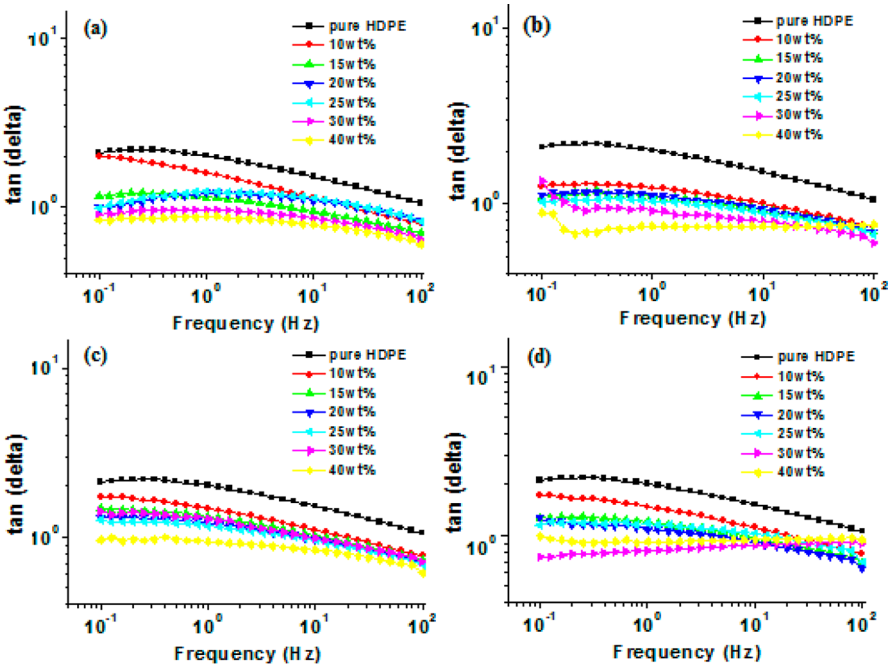

Figure 9. Graphs of tan δ (loss factor) vs frequency for neat HDPE and (a) HDPE/Zn_2Al−Cl LDH nanocomposites, (b) HDPE/Zn_2Al−NO_3 LDH nanocomposites, (c) HDPE/Zn_2Al−CO_3 LDH nanocomposites, and (d) HDPE/Zn_2Al−SO_4 LDH nanocomposites.

the heat and mass transfer between gas and condensed phases and prevents the underlying material from further combustion.[56] The release of abundant gases which dilute the oxygen and the endothermic decomposition might also contribute a lot to the flame retardancy. However, to disclose the detailed mechanism on why different interlayer anions can result in different flame retardant performance needs further investigations.

The HRC is another important parameter usually used to predict and evaluate the fire hazard. The HRC values obtained as a sum of all PHRR values are summarized in Table 2 as well. Neat HDPE exhibit the highest HRC of 1540 J g^{-1} K^{-1}. After adding LDHs, this value is decreased rapidly with increasing the LDH loadings For instance, with 10, 15, 20, 25, 30, and 40 wt % Zn_2Al-SO_4 LDH, the HRC of the nanocomposites is decreased to 1224, 1070, 975, 886, 847, and 669 J g^{-1} K^{-1}, respectively. Similar to PHHR, the influence of interlayer anions on the efficiency of flame retardancy also follows the order of SO_4^{2-} > NO_3^- > CO_3^{2-} > Cl^-. With 40 wt % Zn_2Al−Cl, Zn_2Al-CO_3, Zn_2Al−NO_3, and Zn_2Al−SO_4 LDHs, the value of HRC was 1079, 850, 749, and 669 J g^{-1} K^{-1}, respectively. These results also suggest that Zn_2Al−X LDHs are highly efficient flame retardant nanofillers and the interlayer anion is demonstrated to be one of the key influencing parameters.

THR, which determines how big a fire could be, is another important parameter for fire hazard evaluation. Once the ignition takes place, THR steadily increases with burning time and attains a steady state before the flameout occurs. Thus, for an efficient flame retardant filler, it should be able to reduce THR effectively when it is incorporated into a polymer.[34] As it can be seen in Table 2, THR is significantly reduced with increasing the LDH loading. For example, compared to the THR value of 41.5 kJ g^{-1} in neat HDPE, HDPE/Zn_2Al−SO_4 LDH nanocomposites with a LDH loading of 10, 15, 20, 25, 30, and 40 wt % show a THR value of 37.1, 35.7, 33.8, 31.7, 30.6, and 25.8 kJ g^{-1}, respectively. Considered the fact that LDH cannot be burned to release heat, the calculated THR for the above HDPE/Zn_2Al−SO_4 LDH nanocomposites is 37.7, 36.1, 34.6, 33.2, 31.9, and 29.6 kJ g^{-1}, respectively. These results clearly indicate that the LDH as flame retardant nanofillers for HDPE can effectively decrease the THR value of the nanocomposites.[57] The HRC value obtained as a sum of all peak HRR values is also important for fire hazard evaluation. Similar to THR, the HRC is also significantly reduced after adding LDHs. With 40 wt % Zn_2Al−SO_4 LDH, the HRC is decreased from 1540 J g^{-1} K^{-1} for neat HDPE to 669 J g^{-1} K^{-1}. This value is also much lower than the calculated amount of 1100 J g^{-1} K^{-1} considering that LDH does not contribute to HRC. This result also confirms that LDH is very efficient as a flame retardant for HDPE.

The rheological behavior of the polymer nanocomposites melts are very important for industrial processing.[58] Also, the properties can be detected by characterizing the storage modulus (G′) and loss modulus (G″) as a function of frequency.[59−61] Figures 7 and 8 shows the G′ and G″ as a function of frequency for pure HDPE and its nanocomposites melts. In general, both G′ and G″ increase with increasing the LDH loading, particularly at low frequencies. However, at high frequencies, the effect of the particle loading on the rheological behavior is relatively weak. This phenomenon indicates that the LDHs are not effective to affect the short-range dynamics of the HDPE chains.[62] Different from the viscous liquid behavior of neat HDPE and other nanocomposite melts, a plateau was observed in the low frequency range for the 40 wt % HDPE/Zn_2Al−SO_4 nanocomposite melts, indicating an elastic solid-like behavior. By comparing the G′ and G″ at low frequency region, the influence of interlayer anions on G′ and G″ follows the order of SO_4^{2-} > CO_3^{2-} > Cl^- > NO_3^-, suggesting that different interlayer anions could result in different rheological properties as well. One interesting phenomenon is that the influence of interlayer anions on flame retardancy is exactly the same as on G′ and G″, although the intrinsic reason for such correlation is still unclear so far.

Figure 9 shows the mechanical loss factor (tan δ) as a function of frequency. tan δ is the ratio of loss modulus to storage modulus, which is highly related to the applied frequency. With Zn_2Al−Cl and Zn_2Al−CO_3 as nanofillers, tan δ is decreased with

dx.doi.org/10.1021/am500265a | ACS Appl. Mater. Interfaces 2014, 6, 5094−5104

increasing the LDH loading (see Figure 9a,c). While with Zn_2Al-NO_3 and Zn_2Al-SO_4 as nanofillers, tan δ first decreases with increasing the LDH from 10 to 30 wt % and then starts to increase with 40 wt % LDH. The tan δ of all the nanocomposites shows three different stages: rubbery, viscoelastic, and glassy states.[63] It was reported that the incorporation of LDH nanoparticles restrains the relative motion of the polymer chain and makes the nanocomposites "stiffer".[58,63−65]

4. CONCLUSIONS

In this contribution, a series of environmental friendly and highly efficient flame retardant HDPE nanocomposites has been prepared with inorgano-LDH as nanofillers using the solvent mixing method and investigated for the thermal stability, flame retardancy behavior, and rheological behaviors. XRD and SEM analysis indicated that LDHs were successfully introduced into HDPE matrix using the solvent mixing method. TGA analysis showed that the thermal stability of HDPE can be significantly increased by adding LDHs and the highest temperature increase in $T_{0.5}$ was 67 °C achieved by adding 15 wt % Zn_2Al-Cl LDH. The MCC-2 analysis confirmed that the addition of Zn_2Al-X LDHs can enhance the flame retardant performance of HDPE, and the efficiency was highly dependent on the type of interlayer anions. With 40 wt % LDH, the PHRR reduction for the HDPE/Zn_2Al-Cl, HDPE/Zn_2Al-CO_3, HDPE/Zn_2Al-NO_3, and HDPE/Zn_2Al-SO_4 LDH nanocomposites was 24, 41, 48, and 54%, respectively. Both THR and HRC were also significantly reduced after introducing LDHs. The melt rheological behaviors of all the HDPE/Zn_2Al-X nanocomposites including G′, G″, and tan δ were also evaluated. The thermal stability, flame retardancy, and rheological behaviors of the HDPE/Zn_2Al-X nanocomposites are observed to highly depend on the type of interlayer anions. Thus, for practical applications of this type of nanocomposites, a proper selection of the interlayer anions and an optimization of the chemical composition are highly desired.

AUTHOR INFORMATION

Corresponding Authors

*E-mail: zhanhu.guo@lamar.edu, nanomaterials2000@gmail.com. Phone: +1 4098807654.

*E-mail: qiang.wang.ox@gmail.com, qiangwang@bjfu.edu.cn. Phone: +86 13699130626.

Notes

The authors declare no competing financial interest.

ACKNOWLEDGMENTS

This work is supported by the Fundamental Research Funds for the Central Universities (Grants BLYJ201402 and TD-JC-2013-3), the Beijing Nova Programme (Grant Z131109000413013), the Program for New Century Excellent Talents in University (Grant NCET-12-0787), the National Natural Science Foundation of China (Grant 51308045), and the Key Laboratory of Functional Inorganic Material Chemistry (Heilongjiang University).

REFERENCES

(1) Costache, M. C.; Heidecker, M. J.; Manias, E.; Camino, G.; Frache, A.; Beyer, G.; Gupta, R. K.; Wilkie, C. A. The Influence of Carbon Nanotubes, Organically Modified Montmorillonites and Layered Double Hydroxides on the Thermal Degradation and Fire Retardancy of Polyethylene, Ethylene-vinyl Acetate Copolymer and Polystyrene. *Polymer* **2007**, *48* (22), 6532−6545.

(2) Cao, Z.; Zhang, Y.; Zhao, L.; Peng, M.; Fang, Z.; Klatt, M. Improving the Flame Retardancy and Mechanical Properties of High-density Polyethylene-g-maleic Anhydride with a Novel Organic Metal Phosphonate. *J. Anal. Appl. Pyrol.* **2013**, *102*, 154−160.

(3) Liu, Y.; Cao, Z.; Zhang, Y.; Fang, Z. Synthesis of Cerium N-Morpholinomethylphosphonic Acid and Its Flame Retardant Application in High Density Polyethylene. *Ind. Eng. Chem. Res.* **2013**, *52* (15), 5334−5340.

(4) Faghihi, J.; Morshedian, J.; Ahmadi, S. Effect of Alumina Trihydrate and Borax on Fire Retardancy and Mechanical Properties of High Density Polyethylene (HDPE) Compounds. *Polym. Polym. Compos.* **2010**, *18* (2), 113−122.

(5) Cai, Y.; Hu, Y.; Song, L.; Tang, Y.; Yang, R.; Zhang, Y.; Chen, Z.; Fan, W. Flammability and Thermal Properties of High Density Polyethylene/Paraffin Hybrid as a Form-stable Phase Change Material. *J. Appl. Polym. Sci.* **2006**, *99* (4), 1320−1327.

(6) Jia, S.; Zhang, Z.; Du, Z.; Teng, R.; Wang, Z. A Study of the Dynamic Flammability of Radiation Cross-Linked Flame-Retardant HDPE/EPDM/Silicon-Elastomer Compound. *Radiat. Phys. Chem.* **2003**, *66*, 349−355.

(7) Wang, L.; He, X.; Lu, H.; Feng, J.; Xie, X.; Su, S.; Wilkie, C. A. Flame Retardancy of Polypropylene (nano)Composites Containing LDH and Zinc Borate. *Polym. Adv. Technol.* **2011**, *22*, 1131−1138.

(8) Zhang, G.; Ding, P.; Zhang, M.; Qu, B. Synergistic Effects of Layered Double Hydroxide with Hyperfine Magnesium Hydroxide in Halogen-Free Flame Retardant EVA/HFMH/LDH Nanocomposites. *Polym. Degrad. Stab.* **2007**, *92* (9), 1715−1720.

(9) Marosfoi, B. B.; Garas, S.; Bodzayl, B. Flame Retardancy Study on Magnesium Hydroxide Associated with Clays of Different Morphology in Polypropylene Matrix. *Polym. Adv. Technol.* **2008**, *19*, 693−700.

(10) Laoutid, F.; Bonnaud, L.; Alexandre, M.; Lopez-Cuesta, J. M.; Dubois, P. New Prospects in Flame Retardant Polymer Materials:From Fundamentals to Nanocomposites. *Mater. Sci. Eng. R* **2009**, *63*, 100−125.

(11) Wang, Q.; Undrell, J. P.; Gao, Y.; Cai, G.; Buffet, J.-C.; Wilkie, C. A.; O' Hare, D. Synthesis of Flame-Retardant Polypropylene/LDH-borate Nanocomposites. *Macromolecules* **2013**, *46*, 6145−6150.

(12) Wang, Q.; O'Hare, D. Recent Advances in the Synthesis and Application of Layered Double Hydroxide(LDH) Nanosheets. *Chem. Rev.* **2012**, *112*, 4124−4155.

(13) Manzi-Nshuti, C.; Wang, D.; Hossenlopp, J. M.; Wilkie, C. A. Aluminum-Containing Layered Double Hydroxides: the Thermal, Mechanical, and Fire Properties of (nano)Composites of Poly(methyl methacrylate). *J. Mater. Chem.* **2008**, *18*, 3091−3102.

(14) Wang, Q.; Tay, H. H.; Zhong, Z.; Luo, J.; Borgna, A. Synthesis of High-Temperature CO_2 Adsorbents from Organo-Layered Double Hydroxides with Markedly Improved CO_2 Capture Capacity. *Energy Environ. Sci.* **2012**, *5*, 7526−7530.

(15) Wang, Q.; Gao, Y.; Luo, J.; Zhong, Z.; Armando, B.; Guo, Z.; O'Hare, D. Synthesis of Nano-Sized Spherical Mg_3Al-CO_3 Layered Double Hydroxide as a High-Temperature CO_2 Adsorbent. *RSC Adv.* **2013**, *3*, 3414−3420.

(16) Gao, Y.; Zhang, Z.; Wu, J.; Yi, X.; Zheng, A.; Umar, A.; O'Hare, D.; Wang, Q. Comprehensive Investigation of CO_2 Adsorption on Mg-Al-CO_3 LDH-Derived Mixed Metal Oxides. *J. Mater. Chem. A* **2013**, *1*, 12782−12790.

(17) Wang, Q.; Luo, J.; Zhong, Z.; Borgna, A. CO_2 Capture by Solid-Adsorbents and Their Applications: Current Status and New Trends. *Energy Environ. Sci.* **2011**, *4*, 42−55.

(18) Wang, Q.; Tay, H. H.; Ng, D. J. W.; Chen, L.; Liu, Y.; Chang, J.; Zhong, Z.; Luo, J.; Borgna, A. The Effect of Trivalent Cations on the Performance of Mg-M-CO_3 Layered Double Hydroxides for High-temperature CO_2 Capture. *ChemSusChem* **2010**, *3*, 965−973.

(19) Wang, Q.; Wu, Z.; Tay, H. H.; Chen, L.; Liu, Y.; Chang, J.; Zhong, Z.; Luo, J.; Borgna, A. High Temperature Adsorption of CO_2 on Mg-Al Hydrotalcite: Effect of the Charge Compensating Anions and the Synthesis pH. *Catal. Today* **2011**, *164*, 198−203.

(20) Wang, Q.; Tay, H. H.; Guo, Z.; Chen, L.; Liu, Y.; Chang, J.; Zhong, Z.; Luo, J.; Borgna, A. Morphology and Composition

Controllable Synthesis of Mg-Al-CO_3 Hydrotalcites by Tuning the Synthesis pH and the CO_2 Capture Capacity. *Appl. Clay Sci.* **2012**, *55*, 18−26.
(21) Wang, Q.; Tay, H. H.; Chen, L.; Liu, Y.; Chang, J.; Zhong, Z.; Luo, J.; Borgna, A. Preparation and CO_2 Capture Capacity of Alkali Metal Carbonates Promoted Hydrotalcite. *J. Nanoeng. Nanomanuf.* **2011**, *1*, 298−303.
(22) Zhao, Y.; Wei, M.; Lu, J.; Wang, Z.; Duan, X. Biotemplated Hierarchical Nanostructure of Layered Double Hydroxides with Improved Photocatalysis Performance. *ACS Nano* **2009**, *3*, 4009−4016.
(23) Xu, X.; Lu, R.; Zhao, X.; Xu, S.; Lei, X.; Zhang, F.; Evans, D. G. Fabrication and Photocatalytic Performance of a $Zn_xCd_{1-x}S$ Solid Solution Prepared by Sulfuration of a Single Layered Double Hydroxide Precursor. *Appl. Catal. B: Environ.* **2011**, *102*, 147−156.
(24) Nyambo, C.; Songtipya, P.; Manias, E.; Jimenez-Gasco, M. M.; Wilkie, C. A. Effect of MgAl-Layered Double Hydroxide Exchanged with Linear Alkyl Carboxylates on Fire-Retardancy of PMMA and PS. *J. Mater. Chem.* **2008**, *18*, 4827−4838.
(25) Manzi-Nshuti, C.; Hossenlopp, J. M.; Wilkie, C. A. Comparative Study on the Flammability of Polyethylene Modified with Commercial Fire Retardants and a Zinc Aluminum Oleate Layered Double Hydroxide. *Polym. Degrad. Stab.* **2009**, *94*, 782−788.
(26) Wang, Q.; Wu, J.; Gao, Y.; Zhang, Z.; Wang, J.; Zhang, X.; Yan, X.; Umar, A.; Guo, Z.; O'Hare, D. Polypropylene/Mg_3Al-tartrazine LDH Nanocomposites with Enhanced Thermal Stability, UV Absorption, and Rheological Properties. *RSC Adv.* **2013**, *3*, 26017−26024.
(27) Xue, T.; Gao, Y.; Zhang, Z.; Umar, A.; Yan, X.; Zhang, X.; Guo, Z.; Wang, Q. Adsorption of Acid Red from Dye Wastewater by Zn_2Al-NO_3 LDHs and the Resource of Adsorbent Sludge as Nanofiller for Polypropylene. *J. Alloys Compd.* **2014**, *587*, 99−104.
(28) Alcantara, A. C. S.; Aranda, P.; Darder, M.; Ruiz-Hitzky, E. Bionanocomposites Based on Alginate-Zein/Layered Double Hydroxide Materials as Drug Delivery Systems. *J. Mater. Chem.* **2010**, *20*, 9495−9504.
(29) Plank, J.; Dai, Z.; Keller, H.; v Hössle, F.; Seidl, W. Fundamental Mechanisms for Polycarboxylate Intercalation into C_3A Hydrate Phases and the Role of Sulfate Present in Cement. *Cem. Concr. Res.* **2010**, *40*, 45−57.
(30) Leroux, F.; Besse, J. P. Polymer Intercalated Layered Double Hydroxide: A New Emerging Class of Nanocomposites. *Chem. Mater.* **2011**, *13*, 3507−3515.
(31) Zammarano, M.; Franceschi, M.; Bellayer, S.; Gilman, J. W.; Meriani, S. Preparation and Flame Resistance Properties of Revolutionary Self-Extinguishing Epoxy Nanocomposites Based on Layered Double Hydroxides. *Polymer* **2005**, *46*, 9314−9328.
(32) Xu, S.; Zhang, L.; Lin, Y.; Li, R.; Zhang, F. Layered Double Hydroxides Used as Flame Retardant for Engineering Plastic Acrylonitrile-Butadiene-Styrene (ABS). *J. Phys. Chem. Solids* **2012**, *73*, 1514−1517.
(33) Evans, D. G.; Duan, X. Preparation of Layered Double Hydroxides and Their Applications as Additives in Polymers, as Precursors to Magnetic Materials and in Biology and Medicine. *Chem. Commun.* **2006**, *5*, 485−496.
(34) Costa, F. R.; Wagenknecht, U.; Heinrich, G. LDPE/Mg-Al Layered Double Hydroxide Nanocomposite: Thermal and Flammability Properties. *Polym. Degrad. Stab.* **2007**, *92*, 1813−1823.
(35) Camino, G.; Maffezzoli, A.; Braglia, M.; Lazzaro, M. D.; Zammarano, M. Effect of Hydroxides and Hydroxycarbonate Structure on Fire Retardant Effectiveness and Mechanical Properties in Ethylene-vinyl Acetate Copolymer. *Polym. Degrad. Stab.* **2001**, *74*, 457−464.
(36) Ye, L.; Wu, Q. Effects of an Intercalating Agent on the Morphology and Thermal and Flame-Retardant Properties of Low-density Polyethylene/Layered Double Hydroxide Nanocomposites Prepared by Melt Intercalation. *J. Appl. Polym. Sci.* **2012**, *123* (1), 316−323.
(37) Chen, W.; Qu, B. LLDPE/ZnAl LDH-Exfoliated Nanocomposites: Effects of Nanolayers on Thermal and Mechanical Properties. *J. Mater. Chem.* **2004**, *14*, 1705−1710.
(38) Manzi-Nshuti, C.; Songtipya, P.; Manias, E.; Jimenez-Gasco, M. M.; Hossenlopp, J. M.; Wilkie, C. A. Polymer Nanocomposites Using Zinc Aluminum and Magnesium Aluminum Oleate Layered Double Hydroxides: Effects of LDH Divalent Metals on Dispersion, Thermal, Mechanical and Fire Performance in Various Polymers. *Polymer* **2009**, *50*, 3564−3574.
(39) Manzi-Nshuti, C.; Songtipya, P.; Manias, E.; Jimenez-Gasco, M. M.; Hossenlopp, J. M.; Wilkie, C. A. Polymer Nanocomposites Using Zinc Aluminum and Magnesium Aluminum Oleate Layered Double Hydroxides: Effects of the Polymeric Compatibilizer and of Composition on the Thermal and Fire Properties of PP/LDH Nanocomposites. *Polym. Degrad. Stab.* **2009**, *94*, 2042−2054.
(40) Manzi-Nshuti, C.; Wang, D.; Hossenlopp, J. M.; Wilkie, C. A. The Role of the Trivalent Metal in an LDH: Synthesis, Characterization and Fire Properties of Thermally Stable PMMA/LDH Systems. *Polym. Degrad. Stab.* **2009**, *94* (4), 705−711.
(41) Shi, L.; Li, D.; Wang, J.; Li, S.; Evans, D. G.; Duan, X. Synthesis Flame Retardant and Smoke Suppressant Properties of a Borate-Intercalated Layered Double Hydroxide. *Clays Clay Miner.* **2005**, *53* (3), 294−300.
(42) Ye, L.; Qu, B. Flammability Characteristics and Flame Retardant Mechanism of Phosphate-Intercalated Hydrotalcite in Halogen-Free Flame Retardant EVA Blends. *Polym. Degrad. Stab.* **2008**, *93*, 918−924.
(43) Zhang, Z.; Xu, C.; Qiu, F.; Mei, X.; Lan, B.; Zhang, S. Study on Fire-Retardant Nanocrystalline Mg-Al Layered Double Hydroxides Synthesized by Microwave-Crystallization Method. *Sci. China, Ser. B* **2004**, *47*, 488−498.
(44) Wang, Q.; Zhang, X.; Zhu, J.; Guo, Z.; O'Hare, D. Preparation of Stable Dispersions of Layered Double Hydroxides (LDHs) in Nonpolar Hydrocarbons: New Routes to Polyolefin/LDH Nanocomposites. *Chem. Commun.* **2012**, *48*, 7450−7452.
(45) Wang, Q.; O'Hare, D. Large-Scale Synthesis of Highly Dispersed Layered Double Hydroxide Powders Containing Delaminated Single Layer Nanosheets. *Chem. Commun.* **2013**, *49*, 6301−6303.
(46) Zhang, H.; Wen, X.; Wang, Y. Synthesis and Characterization of Sulfate and Dodecylbenzenesulfonate Intercalated Zinc-Iron Layered Double Hydroxides by One-Step Coprecipitation Route. *J. Solid State Chem.* **2007**, *180*, 1636−1647.
(47) Kono, A.; Miyakawa, N.; Kawadai, S.; Goto, Y.; Maruoka, T.; Yamamoto, M.; Horibe, H. Effect of Cooling Rate After Polymer Melting on Electrical Properties of High-Density Polyethylene/Ni Composites. *Polym. J.* **2010**, *42*, 587−591.
(48) Han, G.; Lei, Y.; Wu, Q.; Kojima, Y.; Suzuki, S. Bamboo-Fiber Filled High Density Polythylene Composites:Effect of Coupling Treatment and Nanoclay. *J. Polym. Environ.* **2008**, *16*, 123−130.
(49) Barus, S.; Zanetti, M.; Lazzari, M.; Costa, L. Preparation of Polymeric Hybrid Nanocomposites Based on PE and Nanosilica. *Polymer* **2009**, *50*, 2595−2600.
(50) Ye, L.; Ding, P.; Zhang, M.; Qu, B. Synergistic Effects of Exfoliated LDH with Some Halogen-Free Flame Retardants in LDPE/EVA/HFMH/LDH Nanocomposites. *J. Appl. Polym. Sci.* **2008**, *107*, 3694−3701.
(51) He, Q.; Yuan, T.; Zhu, J.; Luo, Z.; Haldolaarachchige, N.; Sun, L.; Khasanov, A.; Li, Y.; Young, D. P.; Wei, S.; Guo, Z. Magnetic High Density Polyethylene Nanocomposites Reinforced with In-Situ Synthesized Fe@FeO Core-Shell Nanoparticles. *Polymer* **2012**, *53*, 3642−3652.
(52) Schartel, B.; Pawlowski, K. H.; Lyon, R. E. Pyrolysis Combustion Flow Calorimeter: A Tool to Assess Flame Retarded PC/ABS Materials? *Thermochim. Acta* **2007**, *462*, 1−14.
(53) Ellzey, K. A.; Ranganathan, T.; Zilberman, J.; Coughlin, E. B.; Farris, R. J.; Emrick, T. Novel Deoxybenzoin-Based Polyarylates as Halogen-free Fire-Resistant Polymers. *Macromolecules* **2006**, *39*, 3553−3558.
(54) Hergenrother, P. M.; Thompson, C. M.; Smith, J. G.; Connell, J. W.; Hinkley, J. A.; Lyon, R. E.; Moulton, R. Flame Retardant Aircraft Epoxy Resins Containing Phosphorus. *Polymer* **2005**, *46*, 5012−5024.
(55) Wang, D.; Leuteritz, A.; Wang, Y.; Wagenknecht, U.; Heinrich, G. Preparation and Burning Behaviors of Flame Retarding Biodegradable

Poly (lactic acid) Nanocomposite Based on Zinc Aluminum Layered Double Hydroxide. *Polym. Degrad. Stab.* **2010**, *95*, 2474−2480.
(56) Wang, X.; Zhou, S.; Xing, W.; Yu, B.; Feng, X.; Song, L.; Hu, Y. Self-Assembly of Ni-Fe Layered Double Hydroxide/Graphene Hybrids for Reducing Fire Hazard in Epoxy Composites. *J. Mater. Chem. A* **2013**, *1*, 4383−4390.
(57) Wang, D.; Das, A.; Costa, F. R.; Leuteritz, A.; Wang, Y.; Wagenknecht, U.; Heinrich, G. Synthesis of Organo Cobalt-Aluminum Layered Double Hydroxide via a Novel Single-Step Self-Assembling Method and Its Use as Flame Retardant Nanofiller in PP. *Langmuir* **2010**, *26*, 14162−14169.
(58) Zhu, J.; Wei, S.; Li, Y.; Sun, L.; Haldolaarachchige, N.; Young, D. P.; Southworth, C.; Khasanov, A.; Luo, Z.; Guo, Z. Surfactant-Free Synthesized Magnetic Polypropylene Nanocomposites: Rheological, Electrical, Magnetic and Thermal Properties. *Macromolecules* **2011**, *44*, 4382−4391.
(59) Zhu, J.; Wei, S.; Ryu, J.; Budhathoki, M.; Liang, G.; Guo, Z. In Situ Stabilized Carbon Nanofiber (CNF) Reinforced Epoxy Nanocomposites. *J. Mater. Chem.* **2010**, *20*, 4937−4948.
(60) Zhu, J.; Wei, S.; Yadav, A.; Guo, Z. Rheological Behaviors and Electrical Conductivity of Epoxy Resin Nanocomposites Suspended with In-Situ Stabilized Carbon Nanofibers. *Polymer* **2010**, *51*, 2643−2651.
(61) Mitchell, C. A.; Bahr, J. L.; Arepalli, S.; Tour, J. M.; Krishnamoorti, R. Dispersion of Functionalized Carbon Nanotubes in Polystyrene. *Macromolecules* **2002**, *35*, 8825−8830.
(62) Du, F.; Scogna, R. C.; Zhou, W.; Brand, S.; Fischer, J. E.; Winey, K. I. Nanotube Networks in Polymer Nanocomposites:Rheology and Electrical Conductivity. *Macromolecules* **2004**, *37*, 9048−9055.
(63) Chen, X.; Wei, S.; Yadav, A.; Patil, R.; Zhu, J.; Ximenes, R.; Sun, L.; Guo, Z. Poly(propylene)/Carbon Nanofiber Nanocomposites: Ex Situ Solvent-Assisted Preparation and Analysis of Electrical and Electronic Properties. *Macromol. Mater. Eng.* **2011**, *296*, 434−443.
(64) Wang, Q.; Zhang, X.; Wang, C.; Zhu, J.; Guo, Z.; O'Hare, D. Polypropylene/Layered Double Hydroxide Nanocomposites. *J. Mater. Chem.* **2012**, *22*, 19113−19121.
(65) Li, Y.; Zhu, J.; Wei, S.; Ryu, J.; Sun, L.; Guo, Z. Poly(propylene)/Graphene Nanoplatelet Nanocomposites: Melt Rheological Behavior and Thermal, Electrical, and Electronic Properties. *Macromol. Chem. Phys.* **2011**, *212* (18), 1951−1959.

NOTE ADDED AFTER ASAP PUBLICATION

This article was published ASAP on March 19, 2014. Since that date, the order of the authors has been revised by agreement of the authors and the Editor. The revised version was published on the web on March 21, 2014.